A study of chemical diffusion on a stepped surface by the transition-type-dependent Monte Carlo method

1996 J. Phys.: Condens. Matter 8 4867

(http://iopscience.iop.org/0953-8984/8/27/001)

J. Phys.: Condens. Matter **8** (1996) 4867–4879. Printed in the UK

A study of chemical diffusion on a stepped surface by the transition-type-dependent Monte Carlo method

Min Qiu‡, Pei-Lin Cao†‡ and Jin-hao Ruan‡

† China Centre of Advanced Science and Technology (World Laboratory), PO Box 8730, Beijing 100080, Peoples Republic of China

‡ Department of Physics and State Key Laboratory of High Purity Silicon, Zhejiang University, Hangzhou 310027, Peoples Republic of China

Received 27 November 1995, in final form 20 February 1996

Abstract. Using the lattice gas model and the transition-type-dependent Monte Carlo method, we calculated the chemical surface diffusion coefficients on a stepped surface. We assume that the step exerts an attraction or repulsion on adsorbed particles (adparticles) that occupy the up or down step sites, but no interactions between adparticles. Two kinds of activation energy, calculated from the harmonic potential and from the difference between the saddle-point and single-site energy, are used in our calculation. The calculated results show that perpendicular diffusion decreases greatly with increase in step repulsion and attraction at all coverages. However, for diffusion parallel to the steps, completely different results are obtained for these two calculation methods. If the energy barrier is calculated by the harmonic potential, diffusion parallel to the steps is both coverage and step independent. If the energy barrier is calculated by the second method, diffusion parallel to the steps is greatly enhanced with increase in the step repulsion and attraction at middle or high coverages but decreases slightly at low coverages. The calculated results explain the chemical diffusion anisotropy on a stepped surface. The results also show that the popular harmonic potential method may be not suitable for explaining the experiments where diffusion along step edges may be more rapid than on a flat surface.

1. Introduction

The diffusion of adsorbed atoms or molecules on a solid surface plays an important role in many surface phenomena such as film and crystal growth, heterogeneous catalysis, corrosion, etc [1, 2]. In previous work, most emphasis has been on the perfect surface. As is well known, even single-crystal surfaces are never perfectly flat but contain surface steps, which could affect adsorption [3]. Hence, it is very important to study diffusion on an imperfect surface, especially on a stepped surface.

A variety of experimental techniques are used to examine stepped-surface diffusion. In most studies the field emission fluctuation method [4–6] as well as field ion microscopy [7–9] were used. All these workers found that diffusion on stepped surfaces has anisotropy, and diffusion along the steps generally is greater than the diffusion through the steps, i.e. diffusion is greatly affected by the steps.

Theoretical stepped diffusion studies employ a wide variety of techniques, including the embedded-atom method [10, 11] and the lattice gas (LG) model [12–16]. From such studies it is evident that particle processes on both the up-side and down-side steps play a key role in the detailed understanding of stepped surface diffusion.

0953-8984/96/274867+13$19.50

The LG model is applicable to many problems of surface diffusion. In general, it is too complicated for exact mathematical solution of master equation, but rather easy to 'solve' it by Monte Carlo (MC) simulation, which requires a modest amount of computer resources. The information obtained from MC–LG modelling is enormously useful in providing some insight into the complicated mechanism of surface diffusion.

In the MC–LG model, the self-diffusion coefficient D^*, which is also called the tracer diffusion coefficient, is calculated from the mean square displacement of a tracer particle at zero coverage in the usual way [17].

$$D^* = \lim_{t\to\infty} (\langle r^2(t)\rangle / 4t) \tag{1}$$

where $\langle r^2(t)\rangle$ is the mean square displacement of the ith particle at time t from its initial position at time 0. The response of an adsorber layer to a gradient in chemical potential, most often simply a concentration (coverage) gradient, gives via Fick's law a chemical diffusion coefficient D (sometimes called a collective diffusion coefficient). Estimation D in the course of a MC simulation of LGs is not so simple as estimating a tracer diffusion coefficient [18].

Recently, using the fluctuation method and Kubo–Green method, Uebing and Gomer [12–16] have studied the diffusion coefficient on stepped surfaces. Using the Kubo–Green method, the tracer diffusion coefficient D^* was calculated first; then they calculated the chemical diffusion coefficient D from the relation [12–14, 16]

$$\frac{D}{D^*} = \frac{\langle N\rangle}{\langle (\delta N)^2\rangle}. \tag{2}$$

From [19], we know that this equation is obtained under the assumption that there is no cross correlation between the velocities of different adsorbed particles (adparticles). Their work also showed that the fluctuation and the Kubo–Green methods give identical D-values, even in ordered regions of the phase diagram [15, 16].

Recently, we have proposed a new calculation method in real time using MC simulation and developed a special technique of computation to attain faster convergence [20]. The algorithm is so efficient that the computation difficulties due to 'noise' inherent in the data have been overcome (e.g. in our recent work [21] to determine the efficiency of this algorithm). These developments enable us to calculate the chemical diffusion coefficient directly from Fick's law, but not an approximate relation. For simplification we called this method the transition-type-dependent Monte Carlo (TTDMC) method.

The aim of this paper is to study chemical diffusion on a stepped surface via the TTDMC method. We assumed that the step exerts attraction or repulsion on adparticles, but no interactions between adparticles.

Some work has been carried out on the case in which there is adparticle–adparticle interaction, and the results will be reported elsewhere.

2. Method

The TTDMC [20] simulation, based on a LG model, was performed for a two-dimensional square lattice, with periodic boundary conditions in one direction (say y) and with a stable concentration gradient in the other direction (say x). $L_x \times L_y$ with $L_x = 72$ and $L_y = 30$ were used in these calculations. (The results for 100×50 are almost the same as those for 72×30). Steps are assumed to consist of two adjacent lattice rows, one on the up side and the other on the down side of a lattice step. Adjacent steps are separated by two terrace rows. So there are 18 step groups (one step group including an up-side step, a down-side

step and two terraces) in the square lattice. Descending a step requires a jump from an up-side to a down-side step site and vice versa.

By setting some initial adparticle concentration gradients (e.g. linearly), a stable gradient is assumed to be established if the total number of adparticles in the system and the adparticle current of diffusion fluctuate about an average value. Generally speaking, smooth average concentration curves (versus L_x) will be obtained after (2–4) $\times 10^7$ TTDMC simulations and it will take about 10–20 CPU h on our 486/DX4-*S* computer.

We account for differences between the down-side and up-side step rows by adding (or subtracting) extra adsorption energies E^u_{BS} and E^d_{BS} for adparticles on step rows. In this paper, we assumed that $E^u_{BS} = E^d_{BS} = E_{BS}$ [15].

The binding energy of a typical adparticle to the surface is given by

$$E_{ij} = \begin{cases} E^0_b + E_{BS} & \text{(down-side step rows)} \\ E^0_b - E_{BS} & \text{(up-side step rows)} \\ E^0_b & \text{(terrace rows)} \end{cases} \tag{3}$$

where E_{BS} is the stepped attractive energy or repulsive energy. The binding energy of an isolated adparticle to the substrate is given by E^0_b.

Generally speaking, there are two methods for calculating the activation barrier. One method is from the intersection point of harmonic potential wells centred on adjacent sites, which is defined as [22]

$$E_m = E_{ij,kl} = E^0_m + (E_{ij} - E_{kl})/2 + (E_{ij} - E_{kl})^2/16E^0_m \tag{4}$$

where (i, j) and (k, l) refer to the initial and final sites; the migration barrier for an isolated adparticle is given by E^0_m. The other method is to calculate the energy difference between the saddle-point energy E_0 and single-site energy of the initial site E_{ij} [15]:

$$E_m = E_{ij} - E_0 \tag{5}$$

where E_0 is a constant which represents the binding energy of adparticles at a saddle point and will not be influenced by the steps.

Pictorial representations of these barrier models are shown in figure 1.

We shall discuss the influence of these two different barriers on surface diffusion in detail in section 3 and section 4. In our LG model, migration is allowed only to vacant nearest-neighbour sites [23].

The average concentration on the L_xth column is given by

$$\overline{C}(L_x) = \left(\sum_i n_{L_x} \tau_i \Big/ \sum_i \tau_i \right) \frac{1}{30a^2} \tag{6}$$

where τ_i is the real time interval of the ith TTDMC cycle, n_{Lx} is the number of adparticles in the L_xth column at that time, and a is the nearest-neighbour distance. The particle currents are obtained by the total particles entering the column of $L_x = 72$ divided by the total real-time interval Δt and $30a$. Δt is calculated from [20]

$$\Delta t = \sum \tau_i = \sum \tau^0_i / M$$
$$\tau^0_i = \frac{1}{\nu} \exp\left(\frac{E_m}{k_B T}\right) \tag{7}$$

where M is the total number of possible transition types, E_m is the energy barrier for the ith transition type and $\sum$ represents the sum over all jumps. Then D is obtained from the particle current divided by the negative gradient of concentration:

$$D = -\frac{J}{\mathrm{d}\overline{C}/\mathrm{d}x} = -\frac{N}{(\mathrm{d}\overline{C}/\mathrm{d}x)s\Delta t} \tag{8}$$

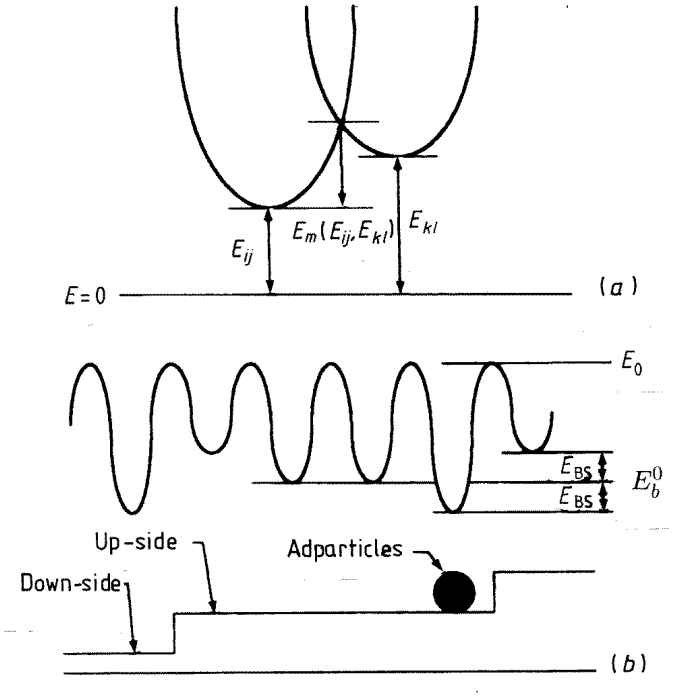

Figure 1. Schematic drawings of the two barrier models: (*a*) model for diffusion barrier described by equation (4); (*b*) model for diffusion barrier described by equation (5).

where N is the total number of particles across the plane with area s (perpendicular to x) in the time interval Δt, and $\overline{C}$ is calculated from equation (6). The advantage of this technique is that, from the profile of the particle concentration, not only the average but also D as functions of concentration (or coverage) are obtained.

3. Results for activation energy calculated from equation (4)

3.1. Coverage of the step and terrace rows

In order to discuss the chemical diffusion it is important to understand the population of the step and terrace. Because there is no interaction between particles, the difference in energy is mainly caused by the repulsion and attraction energy of the step. From equation (3) we know that the binding energy decreases in the order of down-side step, terrace and up-side steps.

Figures 2(*a*), 2(*b*), 2(*c*) and 2(*d*) show representative equilibrium distributions of diffusion adparticles for $E_{BS}/k_BT = 1$, $E_{BS}/k_BT = 2$, $E_{BS}/k_BT = 3$ and $E_{BS}/k_BT = 4$. The results in figure 2 show that the population of the up-side step greatly decreases and the population of the down-side step is enhanced with increase in E_{BS}/k_BT.

The average coverage of a step group is given by

$$\langle\theta\rangle = \frac{\theta_u + \theta_d + \theta_{nu} + \theta_{nd}}{4} \tag{9}$$

where θ_u, θ_d, θ_{nu} and θ_{nd} are the coverages of the up-side step row, the down-side step row, the terrace row of the near-up-side step, and the terrace row of the near-down-side step,

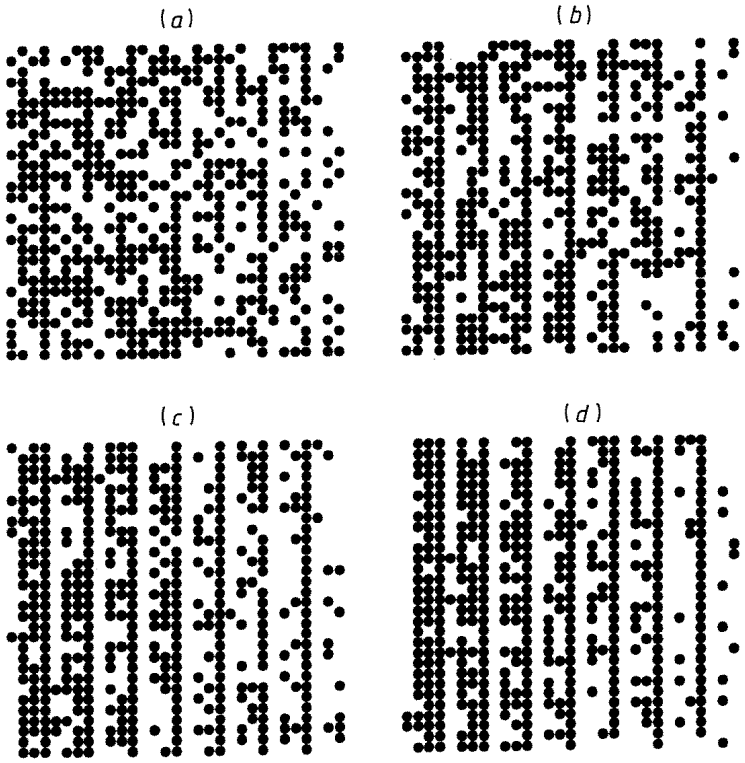

Figure 2. Representative equilibrium distributions of diffusing adparticles near $\theta = 0.5$ for (*a*) $E_{BS}/k_BT = 1$, (*b*) $E_{BS}/k_BT = 2$, (*c*) $E_{BS}/k_BT = 3$ and (*d*) $E_{BS}/k_BT = 4$.

respectively.

Figure 3 shows the relationships between the average coverage $\langle\theta\rangle$ and θ_u, θ_d, θ_{nu} and θ_{nd}. The results show that the coverage decreases in the order of down-side step, terrace and up-side step, just as the binding energy. The difference between the coverage on the up-side and down-side step increases with increase in E_{BS}/k_BT while the coverage of the terrace is near $\langle\theta\rangle$. Because of the absence of interaction between the particles, the binding energy of this site is independent of the number of particles around this site. Hence there is little difference between the coverage on the row near the up-side step and the coverage on the row near the down-side step on the terrace.

The row coverages given in figure 3 are also easily calculated from the Fermi statistics [15]:

$$\ln\left[\frac{\theta_d}{1-\theta_d}\frac{1-\theta_t}{\theta_t}\right] = \frac{E_{BS}}{k_BT} \tag{10}$$

$$\ln\left[\frac{\theta_u}{1-\theta_u}\frac{1-\theta_t}{\theta_t}\right] = -\frac{E_{BS}}{k_BT} \tag{11}$$

where we assume that $\theta_t = \theta_{nu} \approx \theta_{nd}$. The results of MC simulation are in good agreement with the theoretical results.

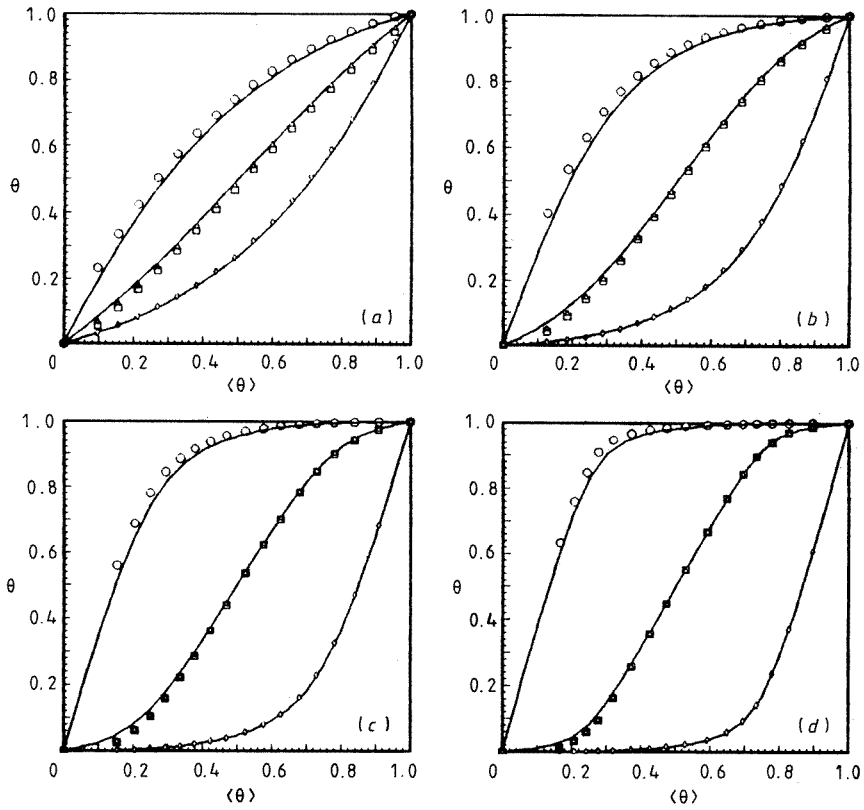

Figure 3. Row coverage θ versus step average coverage $\langle\theta\rangle$ for (*a*) $E_{BS}/k_BT = 1$, (*b*) $E_{BS}/k_BT = 2$, (*c*) $E_{BS}/k_BT = 3$ and (*d*) $E_{BS}/k_BT = 4$: ○, down-side step coverage; ◇, up-side step coverage; △, row adjacent to step, near the up-side step; □, row adjacent to step, near the down-side step. The average coverage is calculated from equation (9). The solid lines are calculated from equations (10) and (11).

3.2. Chemical diffusion coefficient

Now we turn to the relationship between chemical diffusion and the E_{BS}/k_BT. Our calculated results for the average diffusion coefficient $\overline{D}/D_l$ and diffusion coefficients for $\langle\theta\rangle = 0.2$. 0.5, 0.8 are shown in figures 4(*a*), 4(*b*), 4(*c*) and 4(*d*), respectively, in which D_l is the low coverage limit (no steps). Obviously the presence of step repulsion and attraction is of great importance to the chemical diffusion. The results show that the chemical diffusion coefficient ($D_\perp$) which is perpendicular to the step decreases with increase in E_{BS}/k_BT. By the action of the step repulsion and attraction, the binding energy of adparticles in down-side rows increases and that in up-side rows decreases. It is clear from equation (4) that the energy barrier for the jump of adparticles from a down-side to an up-side site increases by more than the amount E_{BS}. With increase in E_{BS}/k_BT, the jump from a down-side to an up-side site becomes the control process for perpendicular diffusion. The larger E_{BS}/k_BT, the smaller $D_\perp$ is, as shown in figure 4. The chemical diffusion coefficient ($D_\parallel$) parallel to the step is almost independent of E_{BS}/k_BT. This is identical with the work by Kutner [24]. In the limit $\theta \to 0$, $D_\parallel$ is equal to D_l.

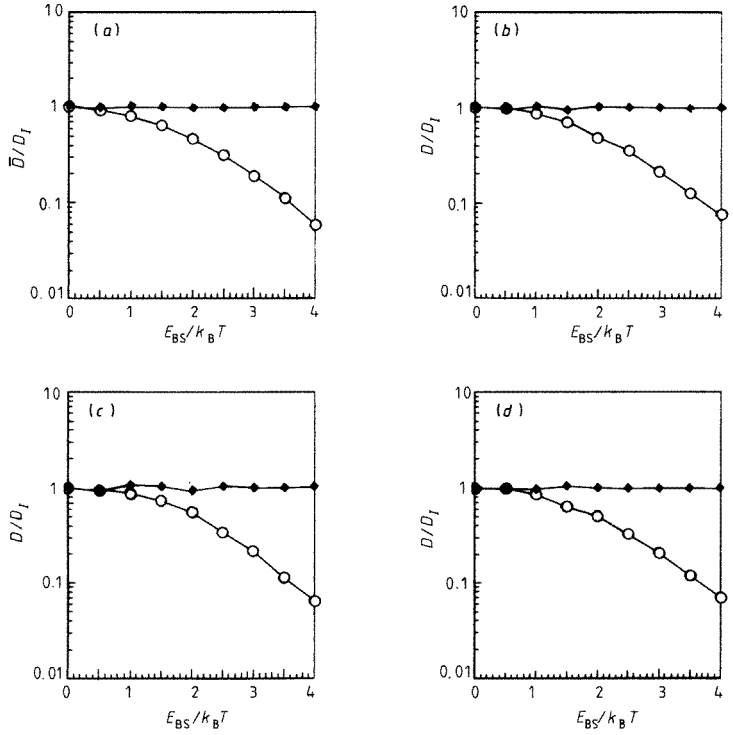

Figure 4. Calculated chemical diffusion coefficients (*a*) $\overline{D}/D_l$ and (*b*)–(*d*) D/D_l ($\bigcirc$, $D_\perp$; $\diamond$, $D_\parallel$) as functions of E_{BS}/k_BT: (*a*) average; (*b*) $\langle\theta\rangle = 0.2$; (*c*) $\langle\theta\rangle = 0.5$; (*d*) $\langle\theta\rangle = 0.8$. The activation energy E_m is calculated from equation (4).

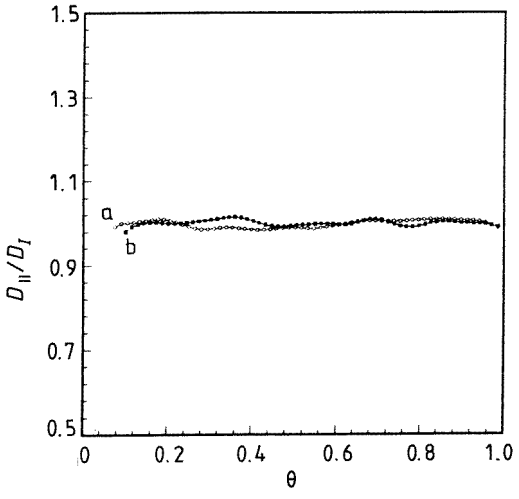

Figure 5. Chemical diffusion coefficients $D_\parallel/D_l$ versus coverage θ: curve a, $E_{BS}/k_BT = 1$; curve b, $E_{BS}/k_BT = 2$. The activation energy E_m is calculated from equation (4).

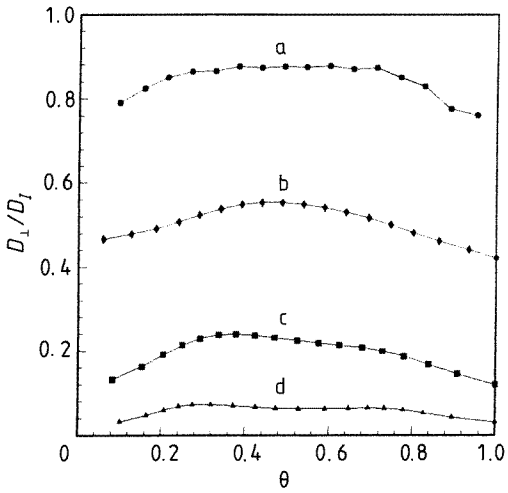

Figure 6. Chemical diffusion coefficient $D_\perp/D_l$ versus average coverage θ: curve a, $E_{BS}/k_BT = 1$; curve b, $E_{BS}/k_BT = 2$; curve c, $E_{BS}/k_BT = 3$; curve d, $E_{BS}/k_BT = 4$. The activation energy E_m is calculated from equation (4).

Figures 5 and 6 show the chemical diffusion coefficients $D_\parallel/D_l$ and $D_\perp/D_l$, respectively, with different E_{BS}/k_BT as functions of coverage. Because the $D_\parallel$ curves are too close to each other, only the curves for $E_{BS}/k_BT = 1$ and $E_{BS}/k_BT = 2$ are shown in figure 5, curves a and b, respectively.

The jumps of adparticles in the same row are responsible for diffusion parallel to the steps. We have already assumed that there is no interaction between adparticles; so from equation (3) we know that E_{ij} and E_{kl} add or subtract E_{BS} at the same time in the same row and, when we calculate the activation energy E_m from equation (4), the activation barrier E_m is constant in this case. So $D_\parallel$ is almost the same as the chemical diffusion coefficient on a flat surface. As expected, parallel diffusion is independent of coverage, as shown in figure 5.

Figure 6 shows that $D_\perp$ for all the coverages decreases with increase in E_{BS}/k_BT, causing a decrease in the average perpendicular diffusion coefficients in figure 4(a). As the coverage increases from zero to 1.0, $D_\perp$ firstly increases and then decreases as shown in figure 6. We shall discuss this problem in detail below. When $\theta \to 0$, the result shows that $D_\perp$ also decreases with increase in E_{BS}/k_BT.

4. Results for activation energy calculated from equation (5)

4.1. Coverages of step and terrace rows

Figure 7 shows the row coverage θ versus E_{BS}/k_BT for various average θ. The results in figure 7 are similar to those in figure 2 of [15] and are also consistent with the results in figure 3 in this paper. Thus two general facts stand out: firstly the density distribution for an equilibrium distribution of diffusing adparticles is independent of the MC simulation method and is also independent of the method for calculating the energy barrier; secondly the distribution depends only on the binding energy of the surfaces sites.

As expected, the calculated results of the relationships between the average coverage

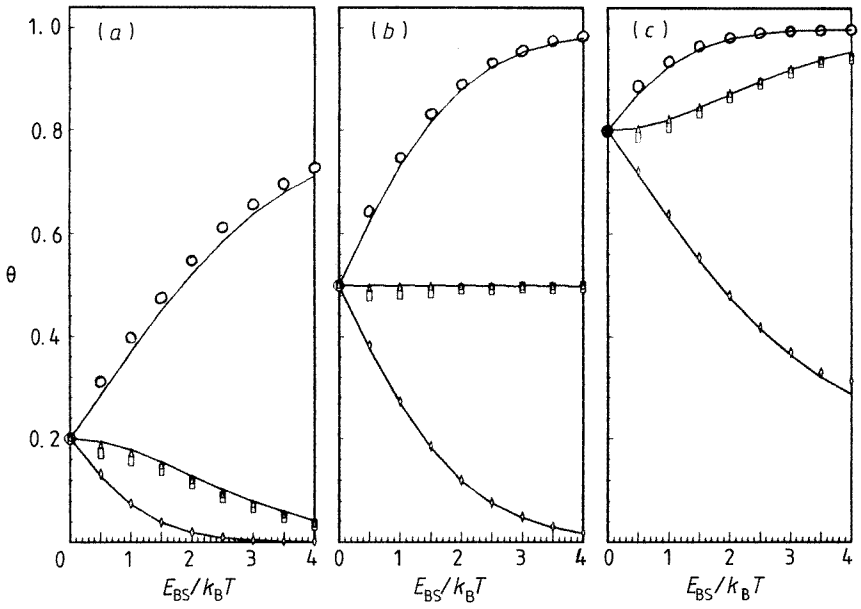

Figure 7. Row coverage θ versus E_{BS}/k_BT for various average θ: (*a*) $\langle\theta\rangle = 0.2$; (*b*) $\langle\theta\rangle = 0.5$; (*c*) $\langle\theta\rangle = 0.8$. All symbols are as in figure 2. The solid lines are calculated from equations (10) and (11). The activation energy E_m is calculated from equation (5).

and θ_u, θ_d, θ_{nu} and θ_{nd} are almost the same as in figure 3. So, in section 4, we shall use the results in figure 3 directly.

4.2. Chemical diffusion coefficient

The calculated chemical diffusion coefficient and its components versus E_{BS}/k_BT are shown in figure 8. Just like the results in figure 4, $D_\perp$ decreases with increase in E_{BS}/k_BT. This is reasonable because the energy barrier from the down-side to the up-side site increases by the amount E_{BS}. As mentioned above, with increase in E_{BS}/k_BT, the jump of adparticles from a down-side to an up-side site becomes the control process for perpendicular diffusion. Comparing our results with those in [15], we find that, for $\langle\theta\rangle = 0.8$, their $D_\perp$ increases with increase in E_{BS}/k_BT. It is obviously unreasonable. It seems that, at high coverages their method will fail because of the assumption of no cross correlation between the velocities of different adparticles as mentioned above.

It is interesting to note that, except for small $\langle\theta\rangle$, $D_\parallel$ increases with increase in E_{BS}/k_BT now. As shown in figure 7, by the action of step repulsion, some adparticles still occupy the up-side rows if $\langle\theta\rangle$ is not very small. We can learn from equation (5) that the activation barrier for the jump along the up-side row is smaller than that on the flat surface. Then the up-side rows become the rapid channel for parallel diffusion as discussed in [15]. For small $\langle\theta\rangle$, $D_\parallel$ first increases and then decreases at large E_{BS}/k_BT. We shall discuss this in detail below.

The experimental results in [25, 26] show that diffusion along step edges may be more rapid in some cases than on flat terraces. Therefore the results shown in figure 8 are in good agreement with the experimental results. We think that, when studying the chemical

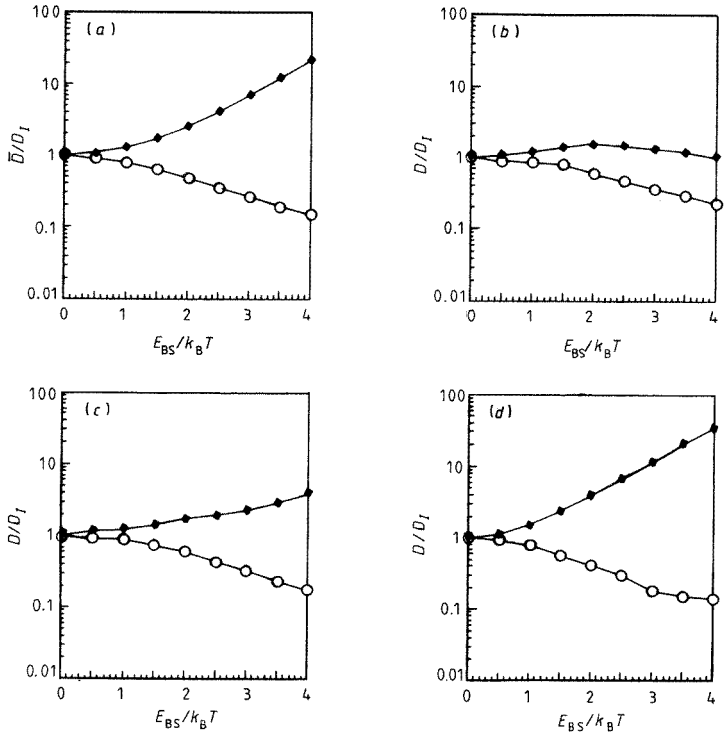

Figure 8. Calculated chemical diffusion coefficients (*a*) $\overline{D}/D_l$ and (*b*)–(*d*) D/D_l (○ , $D_\perp$; ◇, $D_\parallel$) as functions of E_{BS}/k_BT: (*a*) average; (*b*) $\langle\theta\rangle = 0.2$; (*c*) $\langle\theta\rangle = 0.5$; (*d*) $\langle\theta\rangle = 0.8$. The activation energy E_m is calculated from equation (5).

diffusion with no adparticle–adparticle interaction stepped surface, using equation (5) to calculate the activation energy may be more reasonable.

Figures 9 and 10 show the chemical diffusion coefficients $D_\parallel/D_l$ and $D_\perp/D_l$, respectively, as functions of average coverage with different E_{BS}/k_BT. It is evident from figure 9 that $D_\parallel$ increases with increase in coverage. As discussed above, up-side rows are the rapid channel of parallel diffusion. As shown in figure 3, the coverage in up-side rows increases with increase in the average coverage, thus increasing parallel diffusion. The activation barrier along up-side rows decreases with increase in E_{BS}/k_BT, making parallel diffusion stronger, as shown in figure 9 for high average coverage. However, for $\langle\theta\rangle = 0.2$, the diffusion is complicated. $D_\parallel$ first increases slightly and then decreases with increase in E_{BS}/k_BT. As shown in figures 3 and 7, few adparticles still stay in up-side rows for large E_{BS}/k_BT, and are trapped in the down-side rows. The activation barrier along down-side rows is larger than that on terrace and up-side rows. The depletion of adparticles in up-side rows caused a decrease in $D_\parallel$ in this case, as shown in figure 8(*b*). When θ decreases to zero, $D_\parallel$ is identical with D_l and this is also identical with the result in figure 4.

As for $D_\perp$ shown in figure 10, it is similar to figure 6, except that the decrease in $D_\perp$ with increasing E_{BS}/k_BT is more pronounced in figure 6. As mentioned above, with the step repulsion and attraction, the jump from a down-side to an up-side row is the controlling process in perpendicular diffusion. The energy barrier for this jump calculated

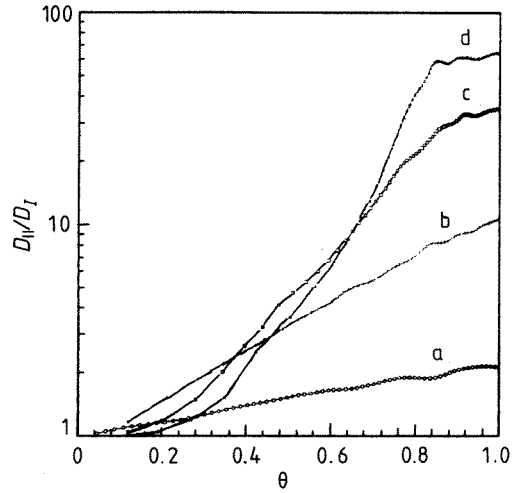

Figure 9. Chemical diffusion $D_{\|}/D_l$ versus coverage θ: curve a, $E_{BS}/k_BT = 1$; curve b, $E_{BS}/k_BT = 2$; curve c, $E_{BS}/k_BT = 3$; curve d, $E_{BS}/k_BT = 4$. The activation energy E_m is calculated from equation (5).

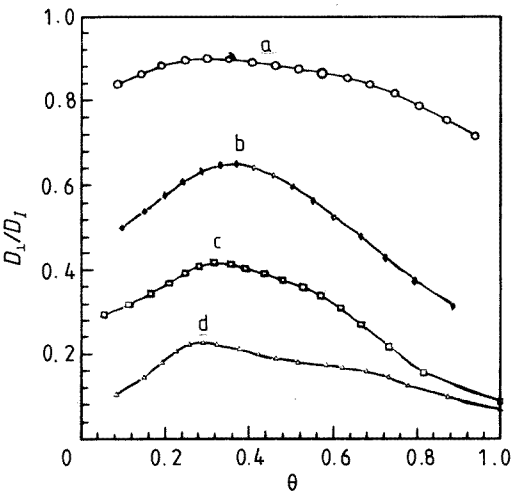

Figure 10. Chemical diffusion $D_{\perp}/D_l$ versus coverage θ: curve a, $E_{BS}/k_BT = 1$; curve b, $E_{BS}/k_BT = 2$; curve c, $E_{BS}/k_BT = 3$; curve d, $E_{BS}/k_BT = 4$. The activation energy E_m is calculated from equation (5).

from equation (4) is larger than that from equation (5), causing a more significant decrease in $D_{\perp}$ with increase in E_{BS}/k_BT in figure 6. At low average coverages, with step attraction and repulsion, almost all the adparticles are trapped in down-side rows, and the coverage of up-side rows is near zero. This suppresses the jump in down-side rows, and enhances the jump from down-side to up-side rows, i.e. enhances perpendicular diffusion. As the average coverage increases further, the down-side rows become saturated and at the same time the number of adparticles in the up-side rows starts to increase, blocking the jump

of adparticles from down-side to up-side rows, i.e. decreasing perpendicular diffusion, as shown in figures 6 and 10. We think that $\theta_d = 0.9$ indicates saturation of down-side rows, i.e. $D_\perp$ reaches its maximum. The results in figure 3 show that, on increase in E_{BS}/k_BT, the point $\theta_d = 0.9$ moves to a low average coverage. This implies that the maximum of $D_\perp$ also moves to a low average coverage on increase in E_{BS}/k_BT. This is in good agreement with the results in figures 6 and 10. Certainly, in the limit $\theta \to 0$, they are also identical.

5. Summary

In this paper, we have studied chemical diffusion on a stepped surface with step attraction and repulsion. The present work shows that the density distribution for an equilibrium distribution of diffusing adparticles is independent of the MC simulation method and also independent of the method used calculate the energy barrier. The distribution depends only on the binding energy of the surface site. The chemical diffusion coefficient depends on the attraction and repulsion energy of steps. Perpendicular diffusion decreases greatly on increase in step repulsion and attraction at all coverages. Parallel diffusion is both coverage and step independent in the case of the energy barrier calculated from the harmonic potential. If the energy barrier is calculated by the saddle-point method, parallel diffusion is greatly enhanced on increase in step repulsion and attraction at middle or high coverages but decreases slightly at low coverages. This paper also shows that, when studying the chemical diffusion on the stepped surface with no adparticle–adparticle interaction, using equation (5) to calculate the activation energy may be more reasonable.

Acknowledgment

This work was supported by the National Science Foundation of China.

References

[1] Schwoebel R L 1969 *J. Appl. Phys.* **40** 614
[2] Henderson M A, Szabo A and Yates J T Jr 1989 *J. Chem. Phys.* **91** 7245 and references therein
[3] Adsorption studies on stepped surfaces were reviewed by Wagner H 1979 *Solid Surface Physics (Springer Tracts Mod. Phys. 85)* ed G Höhler (Berlin: Springer) p 151
[4] Choi D S, Kim S K and Gomer R 1990 *Surf. Sci.* **234** 262
[5] Choi D S, Uebing C and Gomer R 1991 *Surf. Sci.* **259** 139
[6] Uebing C and Gomer R 1991 *Surf. Sci.* **259** 151
[7] Fink H W and Ehrlich G 1986 *Surf. Sci.* **173** 128
[8] Wang S C and Ehrlich G 1991 *Phys. Rev. Lett.* **67** 2509
[9] Wang S C and Ehrlich G 1993 *Phys. Rev. Lett.* **70** 41
[10] Stoltze P and Nørskov J K 1993 *Phys. Rev.* B **48** 5607
[11] Liu C L and Adams J B 1993 *Surf. Sci.* **294** 197
[12] Uebing C and Gomer R 1994 *Surf. Sci.* **306** 419
[13] Uebing C and Gomer R 1994 *Surf. Sci.* **306** 427
[14] Uebing C and Gomer R 1994 *Surf. Sci.* **317** 165
[15] Uebing C 1994 *Phys. Rev.* B **49** 13 913
[16] Uebing C and Gomer R 1994 *J. Chem. Phys.* **100** 7759
[17] Mak C H, Anderson H C and George S M 1988 *J. Chem. Phys.* **88** 4052
[18] Kehr K W and Binder K 1983 *Application of the Monte Carlo Methods in Statistical Physics (Top. Cur. Phys. 36)* ed K Binder (Berlin: Springer)
[19] Gomer R 1990 *Rep. Prog. Phys.* **53** 917
[20] Cao P L 1994 *Phys. Rev. Lett.* **73** 2595
[21] Cao P L, Qiu M and Lee L Q 1996 *J. Phys.: Condens. Matter* **8** 1335

[22] Bowler A M and Hood E S 1991 *J. Chem. Phys.* **94** 5162
[23] Ehrlich G 1982 *CRC Crit. Rev. Solid State Mater. Sci.* **10** 391
[24] Kutner R 1981 *Phys. Lett.* **81A** 239
[25] Sneh O and George S M 1994 *J. Chem. Phys.* **101** 3287
[26] Naumovets A G and Vedula Yu S 1985 *Surf. Sci. Rep.* **4** 365 and references therein